

1 Article

2 Clinical Surveillance Identifies SARS-CoV-2 Outbreaks and 3 Emergence of Novel Variants in Real-Time

4 Steven C. Holland¹, ABCTL Diagnostic Testing and Sequencing Teams^{1,2}, Ian Shoemaker¹, Theresa Rosov¹, Caro-
5 line Compton¹, Joshua LaBaer¹, Efrem S. Lim³, and Vel Murugan^{1,4,*}

6 ¹Virginia G. Piper Center for Personalized Diagnostics, Biodesign Institute, Arizona State University, Tempe,
7 Arizona, USA

8 ²ASU Biodesign Clinical Testing Laboratory, Biodesign Institute, Arizona State University, Tempe, Arizona,
9 USA

10 ³Communicable Diseases Agency, Singapore

11 ⁴College of Health Solutions, Arizona State University, Phoenix, Arizona, USA

12 * Correspondence: Vel.Murugan@asu.edu; Tel.: +1 480-727-0402

13 **Abstract:** Monitoring community health and tracking SARS-CoV-2 evolution were criti-
14 cal priorities throughout the COVID-19 pandemic. However, widespread shortages of
15 personal protective equipment, the necessity for social distancing, and the redeployment
16 of healthcare personnel to clinical duties presented significant barriers to traditional
17 sample collection. In this study, we evaluated the feasibility of using self-collected saliva
18 specimens for the qualitative detection of SARS-CoV-2 infection. Following confirmation
19 of reliable viral detection in saliva, we established a large-scale surveillance program in
20 Arizona, USA, to enable clinical diagnosis and genomic sequencing from self-collected
21 samples. Between April 2020 and December 2023, we tested approximately 1.4 million
22 saliva samples using RT-PCR, identifying 94,330 SARS-CoV-2 infections. Whole genome
23 sequencing was performed on 69,595 samples, yielding 54,040 high-quality consensus
24 genomes. This surveillance approach enabled real-time monitoring of infection trends,
25 outbreak detection within specific populations, and the identification of novel viral lin-
26 eages over the course of the pandemic. The co-location of clinical testing and sequencing
27 capabilities within the same facility significantly reduced turnaround time from the
28 identification of positive cases to the generation of sequencing data. Our findings support
29 the use of self-collected saliva as a scalable, cost-effective, and practical strategy for in-
30 fectious disease surveillance in future pandemics.

31 **Keywords:** SARS-CoV-2, public health surveillance, saliva, next generation sequencing,
32 gene target failure

33

34 1. Introduction

35 The novel coronavirus SARS-CoV-2, the causative agent of COVID19 disease, was first
36 observed in Wuhan, China in November 2019 [1]. On January 30, 2020, the World Health
37 Organization (WHO) declared the SARS-CoV-2 virus and COVID19 a public health
38 emergency of international concern (PHEIC) [2]. On May 5, 2023, WHO ended the PHEIC
39 designation of SARS-CoV-2 and COVID19 [3]. Over the three-year public health emer-
40 gency, over 670 million cases of COVID19 and over 6.8 million deaths are estimated to
41 have occurred due to SARS-CoV-2 [4].

42 To diagnose many respiratory infections, the recommended patient sample type is na-
43 sopharyngeal swab (NPS) or nasopharyngeal aspirate (NPA). These sample collection
44 methods are often uncomfortable for patients and usually require collection by a trained
45 healthcare worker, increasing the risk of virus transmission [5]. Because of these consid-
46 erations and lower cost, saliva has been increasingly studied for its value in diagnosing
47 respiratory infection [6]. Throughout the pandemic, saliva was analyzed for its ability to
48 make qualitative, diagnostic assessment of SARS-CoV-2 infection and was found to be a
49 reliable sample matrix [7,8].

50 Early in the pandemic, the US Centers for Disease Control described primer and probe
51 sequences for the detection of SARS-CoV-2 via nucleic acid amplification tests [9]. Shortly
52 after, independently designed commercial nucleic acid amplification tests became
53 available for diagnostic and research use. On March 13, 2020, the TaqPath COVID-19
54 Combo Kit received Emergency Use Authorization (EUA) for detection of SARS-CoV-2 in
55 nasopharyngeal swabs, bronchoalveolar lavage, mid-turbinate swabs, nasal swabs, na-
56 sopharyngeal aspirate, and oropharyngeal swabs [10]. The TaqPath COVID-19 Combo
57 Kit contained primers and probes targeting the SARS-CoV-2 orf-1ab, S, and N genes but
58 the oligo sequences were not publicly available. Evolution of SARS-CoV-2 increasingly
59 led to the discovery of lineages with mutations affecting test sensitivity at one gene locus,
60 termed gene target failure (GTF) [11,12]. On July 30, 2021, the TaqPath COVID-19 Fast
61 PCR Combo Kit 2.0 was designed and granted EUA for use on saliva samples [13]. While
62 exact assay designs are not publicly available, the manufacturer describes that each gene
63 (Orf1a, Orf1b, and N) is interrogated with multiple probes sharing the same fluorescent
64 moiety [14]. With this scheme, multiple mutations within a gene are required for target
65 failure and the highly mutating S gene is no longer a gene target.

66 The SARS-CoV-2 pandemic occurred during, and further bolstered, the increased avail-
67 ability of next generation sequencing (NGS) capabilities. The whole genome sequencing
68 of pathogens can inform public health guidance with regard to the detection novel and
69 recombinant virus lineages containing mutations of health and therapeutic interest. One
70 sequencing strategy used to increase target nucleic acid concentration in samples is tiled
71 amplicon sequencing [15]. This strategy uses primer oligos to PCR amplify the whole
72 target genome across two or more library pools. Like RT-PCR, tiled amplicon sequencing
73 also relies on primer homology to create sequencing amplicons and is also susceptible to
74 viral evolution causing the unsuccessful amplification of some amplicons. The popular
75 ARTIC network protocol uses over 90 amplicons to amplify the approximately 30kb ge-
76 nome of SARS-CoV-2 and the primer scheme was updated multiple times throughout the
77 pandemic to account for mutations in primer regions causing reduced amplification
78 sensitivity [16].

79 With the increased available knowledge of whole genome evolution of the SARS-Cov-2
80 virus provided by NGS, the creation of naming conventions to describe novel viral phy-
81 logenetic lineages below the species level was needed. The PANGO nomenclature system
82 was proposed and adopted to describe virus lineages which contained specific constella-
83 tions of mutations and comprised their own distinct phylogenetic branches [17]. Because
84 this nomenclature captured mostly genotypic information, in 2021, the WHO announced
85 a naming scheme that would supplement PANGO classification in order to highlight
86 PANGO lineages with notable phenotypic traits [18]. To facilitate public health commu-
87 nication, notable lineages would be designated as variants of interest (VOIs) and variants
88 of concern (VOCs) and be given Greek letter labels depending on their transmissibility,
89 virulence, and clinical presentation characteristics. WHO later added a variant under

90 monitoring (VUM) designation, which aimed to raise awareness to lineages based on
91 phylogenetic and genotypic data, before robust phenotypic data was available [19].

92 To assess the epidemiological state and viral evolution of SARS-CoV-2 in Arizona, USA,
93 we established a multi-yearlong study using self-collected saliva samples. Over 1.4 mil-
94 lion RT-PCR assays were performed on saliva samples from over 360,000 participants.
95 Over 94,000 samples tested positive for SARS-CoV-2 infection and over 69,000 samples
96 were subjected to NGS to obtain whole SARS-CoV-2 consensus genomes. Over the sur-
97 vey period, our efforts resulted in the deposition of over 54,000 SARS-CoV-2 consensus
98 genomes into the GISAID database. Due to the robust results and the ease of sample
99 collection, we believe self-administered saliva collection could provide an effective
100 means for analyzing future respiratory disease outbreaks.

101 2. Materials and Methods

102 2.1. Nucleic acid extractions

103 Nucleic acid extractions were performed using the MagMAX Total RNA Isolation
104 Kit (Invitrogen, Waltham, Massachusetts, USA) using a KingFisher Flex (Thermo Scien-
105 tific, Waltham, Massachusetts, USA). Briefly, 200 μL of saliva sample or NP viral transfer
106 medium (VTM) was added to 10 μL of total nucleic acid magnetic beads and 265 μL
107 Binding Solution. For NPS, 400 μL of NPS storage solution was added to 20 μL of total
108 nucleic acid magnetic beads and 530 μL Binding Solution. Sample binding mixes, re-
109 quired buffers, and wash solutions were prepared in 96-well format using a Biomek i7
110 automated liquid handler (Beckman Coulter Life Sciences, Indiana, USA). With the
111 MagMAX instrument loaded with wash solutions, diluted TURBO DNase, and elution
112 buffers as directed by the manufacturer's protocol, the 'MagMAX Total' program was
113 run on the KingFisher Flex. Aliquots of nucleic acid extracts were used for immediate
114 testing and the remainder stored at -80°C .

115 2.2. RT-PCR assays

116 Nucleic acid extracts run on the TaqPath COVID19 Combo Kit (Applied Biosystems;
117 Waltham, Massachusetts, USA) were assayed following the manufacturer's instructions
118 for 384-well format. Assay plates were prepared using a custom automation method on a
119 Biomek i7 automated liquid handler. For saliva samples, 11 μL of nucleic acid extract was
120 used as sample input and combined with 11 μL reconstituted Reaction Mix. For NPS, 5
121 μL of nucleic acid extract was used as sample input and combined with 20 μL reconsti-
122 tuted Reaction Mix. The RT-PCR cycling reactions were performed and analyzed on a
123 QuantStudio7 Flex (Applied Biosystems; Waltham, Massachusetts, USA) instrument
124 with the following cycle conditions: 1 cycle of 25°C for 2 minutes, 53°C for 10 minutes, 1
125 cycle of 95°C for 2 minutes, and 40 cycles of $95^{\circ}\text{C}/60^{\circ}\text{C}$ for 3 seconds/30 seconds. Assay
126 interpretations were performed as per manufacturer's recommendations.

127 Saliva samples run on the TaqPath COVID-19 Fast PCR Combo Kit 2.0 (Applied
128 Biosystems; Waltham, Massachusetts, USA) were assayed following the manufacturer's
129 instructions for 384-well format. Assay plates were prepared using a custom automation
130 method on a Biomek i7 automated liquid handler. Briefly, 22 μL of saliva was added to 22
131 μL SalivaReady and incubated for 5 minutes at 62°C and then 5 minutes at 92°C . Then 14
132 μL of the SalivaReady reaction was combined with 6 μL of reconstituted Assay Reaction
133 Mix. The RT-PCR cycling reactions were performed and analyzed on a QuantStudio7
134 Flex (Applied Biosystems; Waltham, Massachusetts, USA) instrument with the following
135 cycle conditions: 53°C for 5 minutes, 1 cycle of 85°C for 5 minutes, 1 cycle of 95°C for 2

136 minutes, and 40 cycles of 95°C/62°C for 1 second/30 seconds. Assay interpretations were
137 performed as per manufacturer's recommendations.

138 *2.3 Limit of detection and heat stability testing of SARS-CoV-2 in saliva*

139 Heat-inactivated SARS-CoV-2 virus particles were obtained from ATCC (Catalog
140 #VR-1986HK). Three aliquots of virus particles were diluted to 100,000 copies/μL in a
141 pool of SARS-CoV-2 negative saliva from 10 individuals and diluted to 3.1 copies/μL
142 using 2-fold serial dilutions. Sample nucleic acids were extracted using the MagMAX
143 assay and assayed for detection of SARS-CoV-2 using the TaqPath COVID19 Combo Kit.
144 For confirmation of limit of detection, 24 samples at 100,000 SARS-CoV-2 virus parti-
145 cles/μL were generated and serially diluted to 12.5/μL. Sample nucleic acids were ex-
146 tracted using the MagMAX assay and tested for SARS-CoV-2 detection using the TaqPath
147 COVID19 Combo Kit at concentrations 1x, 2x, 4x, 8x, 16x, and 24x the limit of detection.

148 *2.4. Paired NPS and saliva sample collection*

149 Paired saliva and NPS were collected from 148 individuals. NPS were collected by
150 trained nurses and stored in 500 μL VTM. Saliva samples were collected by each partic-
151 ipant. NPS and saliva samples were collected within 30 minutes of each other. NPS and
152 saliva samples had their nucleic acids extracted and assayed for the presence of
153 SARS-CoV-2 using the TaqPath COVID19 Combo Kit as described above.

154 *2.5. Saliva sample kit creation, distribution, collection, and testing*

155 Saliva collection kits were composed of a set of sample collection and registration
156 instructions, an absorbent towel, alcohol wipe, a sample return bag, and a 6 ml collection
157 tube (Micronic, Lelystad, Netherlands) labeled with a 1 ml minimum sample volume and
158 unique tube identifier (ID). Each tube contained two identifiers consisting of a 10-digit
159 numeric and a 5-digit alphanumeric. 5-digit alphanumeric identifier was mathematically
160 derived from the 10-digit. Participants were requested to enter both IDs to verify the in-
161 tegrity of sample IDs, to make sure that the delivery of sample results to the right par-
162 ticipant. Collection kits were placed near sample return locations and distributed to
163 partner institutions.

164 Participants were recruited from partnered private organization employees, gov-
165 ernmental organization employees, university students, and eventually their dependents
166 and families. Recruitment was comprised of self-initiated testing and institution selected
167 testing. Testing frequency and selection method were determined by each institution
168 independently. Depending on availability, the participants were able to choose a super-
169 vised collection site or to drop off a sample at an unsupervised site.

170 From April 4, 2020, until December 2021, supervised self-collected saliva drop-off
171 sites were available. At these locations, trained staff and nurses were available to aid in
172 kit distribution, sample collection, and sample registration. At these locations, deposited
173 samples were maintained at 4°C and were collected every day.

174 For testing after February 2021, unsupervised drop-off sites were created where
175 participants deposited their self-collected samples in sample deposit boxes. Sample de-
176 posit boxes varied but generally were a lockable container having a lid with a hole for
177 sample return. Over the course of the survey period, approximately 40 deposit locations
178 were used. The local conditions of deposit bins varied, and climate-controlled locations
179 were preferred, but the temperatures of deposited samples were not regulated. Partici-
180 pants could drop-off samples 24 hours a day (dependent on location accessibility), and
181 samples were usually collected twice daily.

182 Sample registration occurred when a participant electronically registered their col-
183 lection tube ID to a custom HIPAA-compliant database and sample management soft-

184 ware. Sample registration required participants to enter a 10-digit numeric tube ID and
185 5-digit alphanumeric sequence. The alphanumeric sequence was derived from the
186 10-digit sequence, so successful registration required both sequences to be correctly en-
187 tered, thus minimizing human input error. Saliva samples had nucleic acids extracted
188 and assayed for SARS-CoV-2 infection by RT-PCR. From April 2020 to October 2021, all
189 collected saliva sample extracts were assayed using the TaqPath COVID19 Combo Kit.
190 After October 2021, saliva samples extracts were first analyzed using the TaqPath
191 COVID-19 2.0 assay for diagnosis, and positive samples had their nucleic acids extracted
192 and assayed using the TaqPath COVID19 Combo Kit assay. Sample results were elec-
193 tronically returned after appropriate approval by quality control and assurance officers
194 under CLIA compliant protocols.

195 2.6. Participant demographics curation

196 During online sample registration, participants were asked to self-identify their sex,
197 race, and ethnicity. Participants were also asked to enter their birthday. For each partic-
198 ipant's sex, race, and ethnicity, categorization of a participant was based on concordance
199 of all of a patient's registered samples. To be included as part of a cohort, all of a partic-
200 ipant's samples must have been registered with the same categorization (i.e., Male, Fe-
201 male, Unknown), or provided no response on other sample registrations. If a conflicting
202 answer was provided on at least one tube, then the participant was assigned 'Invalid or
203 no answer' for that categorization. For patient age at first test, the birthdate entered on
204 the first registered sample was used to calculate the participant's age. Ages exceeding 113
205 years were assigned 'Invalid or no answer.'

206 2.7. Next generation sequencing of SARS-CoV-2

207 Sequencing facilities were in the same building where the diagnostic testing was
208 performed. NGS libraries were built on nucleic acid extracts using the COVIDSeq Test
209 (Illumina, San Diego, CA, USA) using ARTICv3, ARTICv4, or ARTICv4.1 [16] primer
210 sets. Libraries were prepared for sequencing using a custom automation method on a
211 Biomek i7 liquid handler. Libraries were sequenced on an Illumina NextSeq2000 using 2
212 x 109 paired end reads. Reads were quality trimmed, filtered, and mapped using a cus-
213 tom pipeline using default parameters on software algorithms up to date at the time of
214 analysis unless noted. Reads were trimmed of adapter sequences using trim-galore [20] (a
215 wrapper for Cutadapt [21] and FastQC [22]) and aligned to the Wuhan1 reference ge-
216 nome (Genbank MN908947.3) using the Burrows-Wheeler aligner, BWA-MEM [23].
217 Primer sequences were removed from reads using iVar (arguments: -e, -q 30) [24] soft-
218 ware. Consensus genomes were created using samtools (arguments: -t 0.60, -m 10, -n N)
219 [25], given lineage assignments using pangolin [26], and validated using VADR (argu-
220 ments: --glsearch, -s, -r, --nomisc, --lowsim5seq 2, --lowsim5ftr 2, --lowsim3seq 2,
221 --lowsim3ftr 2, --alt_pass peptrans, --alt_fail lowscore,fstukcft,insertnn,deletinn) [27].

222 2.8. Statistical analysis

223 LOWESS/LOESS regression and Pearson correlation were calculated using
224 GraphPad Prism software (Insight Partners, New York City, New York, USA). Ellipses
225 generation and Wilson's confidence interval calculation was performed using R software.
226

227 3. Results

228 3.1. Saliva is a stable and reliable sample matrix for SARS-CoV-2 testing

229 To test the feasibility of using saliva as a SARS-CoV-2 sample collection and extrac-
 230 tion matrix, we first assayed the limit of detection on pooled, SARS-CoV-2 negative saliva
 231 samples with known quantities of spiked-in, heat inactivated SARS-CoV-2 virus particles
 232 (Table 1). Using a preliminary sample size of 3 samples per concentration, we obtained
 233 positive results for SARS-CoV-2 in all 3 samples down to 12.2 virus particles/ μ L. In order
 234 to confirm using 12.5 as our lower limit of detection, we expanded the sample size from 3
 235 to 24 samples for a series of low virus concentrations. We successfully detected
 236 SARS-CoV-2 in all samples (24/24) at 1x, 2x, 4x, 8x, 16x, and 32x the lower limit of detec-
 237 tion (Table 1). The ORF1ab and S gene loci appeared to be slightly more sensitive than
 238 the N gene locus, with consistently lower Ct values and detecting SARS-CoV-2 down to
 239 6.1 particles/ μ L in one sample. Limit of detection analysis of NPSs resulted in similar
 240 detection patterns and a lower limit of detection of 1 virus particle per microliter of saliva
 241 (Supplementary Table 1).

242 **Table 1.** Limit of detection for SARS-Cov-2 virus particles in a saliva matrix.

Assay	Virus parti- cles/ μ L saliva	Positive/ Total	RNase P	Average Ct value (St. dev.)		
				ORF1ab	N gene	S gene
Limit of de- tection (LOD)	100000	3/3	21.81 (0.1)	18.31 (0.16)	18.84 (0.17)	18.36 (0.12)
	50000	3/3	21.76 (0.1)	19.46 (0.17)	19.88 (0.06)	19.44 (0.12)
	25000	3/3	21.7 (0.22)	20.45 (0.22)	20.75 (0.06)	20.34 (0.13)
	12500	3/3	21.71 (0.19)	21.4 (0.2)	21.67 (0.18)	21.29 (0.09)
	6250	3/3	21.72 (0.19)	22.14 (0.35)	22.55 (0.12)	22.01 (0.35)
	3125	3/3	21.61 (0.13)	23.11 (0.16)	23.56 (0.19)	23.13 (0.21)
	1562.5	3/3	21.65 (0.04)	24.16 (0.2)	24.46 (0.08)	24.15 (0.18)
	781.3	3/3	21.63 (0.2)	25.28 (0.36)	25.42 (0.19)	25.3 (0.27)
	390.6	3/3	21.68 (0.12)	25.83 (0.2)	26.39 (0.1)	25.89 (0.18)
	195.3	3/3	21.67 (0.11)	27.04 (0.11)	27.48 (0.1)	27.25 (0.07)
	97.7	3/3	21.53 (0.19)	27.59 (0.27)	28.38 (0.16)	27.84 (0.48)
	48.8	3/3	21.53 (0.1)	28.35 (0.57)	29.93 (0.81)	29.76 (0.92)
	24.4	2/3	21.49 (0.25)	30.9 (2.39)	31.99 (0.82)	31.3 (0.77)
	12.2	3/3	21.5 (0.39)	31.68 (0.48)	37.3 (0.82)	35.49 (2.09)
	6.1	1/3	21.62 (0.04)	35.15	-	36.65
3.1	0/3	21.78 (0.21)	-	-	-	
Confirmation	12.5 (1x LOD)	24/24	22.89 (0.22)	30.36 (0.61)	30.78 (0.49)	30.54 (0.75)
	25 (2x LOD)	24/24	22.71 (0.26)	29.35 (0.54)	29.83 (0.55)	29.38 (0.73)
	50 (4x LOD)	24/24	22.68 (0.36)	28.03 (1.3)	28.5 (1.36)	28.08 (1.43)
	100 (8x LOD)	24/24	22.48 (0.7)	26.91 (1.49)	27.65 (0.71)	26.8 (2.17)
	200 (16x LOD)	24/24	22.85 (0.19)	26.25 (0.51)	26.89 (0.24)	26.08 (0.54)
	400 (32x LOD)	24/24	22.78 (0.29)	25.14 (0.92)	26.01 (0.38)	25.03 (0.88)

243 With self-collection there are often delays between saliva collection and sample
 244 processing, so we tested SARS-CoV-2 virus particle detection at different times up to 72
 245 hours at four storage temperatures (Figure 1). At the ORF1ab locus, Ct values deviated
 246 by less than 1 Ct over 72 hours for the -20°C, 4°C, and 20°C samples. There were greater
 247 deviations observed in samples incubated at 42°C, but differences to the initial Ct values
 248 stayed within 2 Ct values. Slightly greater Ct deviations were observed at the N gene and
 249 S gene loci. Overall, the differences we observed at the -20°C and 4°C temperatures de-
 250 viated less than those at incubated at 20°C, and the samples incubated at 42°C showed
 251 the greatest deviations.
 252

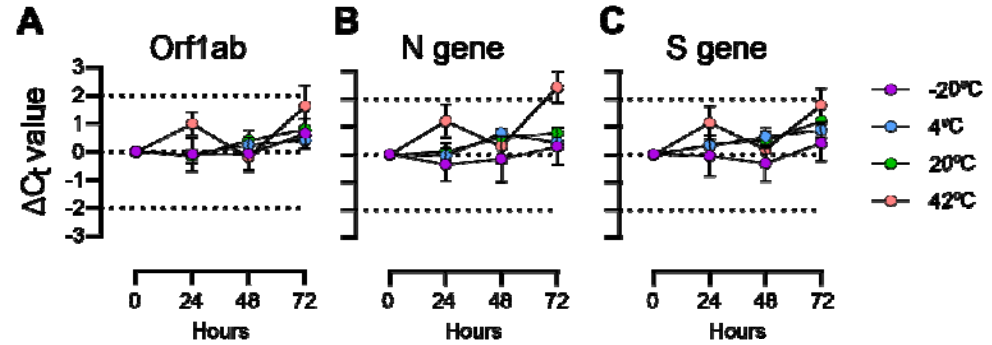


Figure 1. TaqPath Ct differences for saliva samples with spiked-in SARS-CoV-2 particles incubated at four times over 72 hours. (a) Orflab gene primer/probe target; (b) N gene primer/probe target; (c) S gene primer/probe target.

Finally, we wanted to compare the concordance of saliva-based SARS-CoV-2 testing to ‘gold-standard’ NP swab SARS-CoV-2 testing (Table 2). We tested 148 paired NP and saliva samples for SARS-CoV-2 using the TaqPath Combo Kit assay. There was 95% positive concordance (19/20 samples; 95% Wilson’s CI: 76.4%-99.1%) and 99.2% negative concordance (127/128 samples; 95% Wilson’s CI: 95.7%-99.9%) between the two sampling methodologies.

Table 2. Comparison of nasopharyngeal swab (NPS) and saliva sampling method for detection of SARS-CoV-2 infection using the TaqPath COVID-19 Combo Kit qPCR assay.

		NPS	
		Positive	Negative
Saliva	Positive	19	1
	Negative	1	127
	Total	20	128

With the finding that SARS-CoV-2 could be stably detected in saliva with good concordance to NP swab testing, we continued with large-scale self-administered saliva collection and RT-PCR SARS-CoV-2 surveillance.

3.2. Participant demographics of saliva-based COVID-19 surveillance

From April 2, 2020, to December 31, 2023, 1434873 SARS-CoV-2 RT-PCR assays were performed on participant-collected saliva samples (Table 3). Over the surveillance period, 94,330 (6.6%) samples tested positive for SARS-CoV-2 and 10,922 (0.8%) samples were invalid. Most samples were collected from three Arizona counties: Maricopa County (74.5%), followed by Coconino County (15.8%), and Pima County (6.3%), with the remaining samples (3.2%) coming from other counties. There were 366,681 unique participants who provided saliva samples. Slightly more participants identified as male (50.7%) than female (48.2%). Most participants identified as white (55.2%), but a large portion of participants provided an invalid answer or no answer (16.2%). A sizable portion of participants identified Hispanic or Latino ethnicity (21.9%). Most participants were aged 18-21 (21%) at the time of their first collection, indicating that college-aged students have a high representation in the participant set.

Table 3. SARS-CoV-2 RT-PCR and NGS assays performed from April 2020 to December 2023.

	No.	%
--	-----	---

Total tests	1434873	
Negative tests	1329621	92.7%
Positive tests	94330	6.6%
NGS sequenced	69595	73.8% ¹
Deposited into GISAID	54040	77.6% ²
Invalid tests	10922	0.8%

¹Percentage of RT-PCR positive samples. ²Percentage of NGS sequenced samples.

283

284

285

Table 4. Demographics of surveillance participants from April 2020 to December 2023.

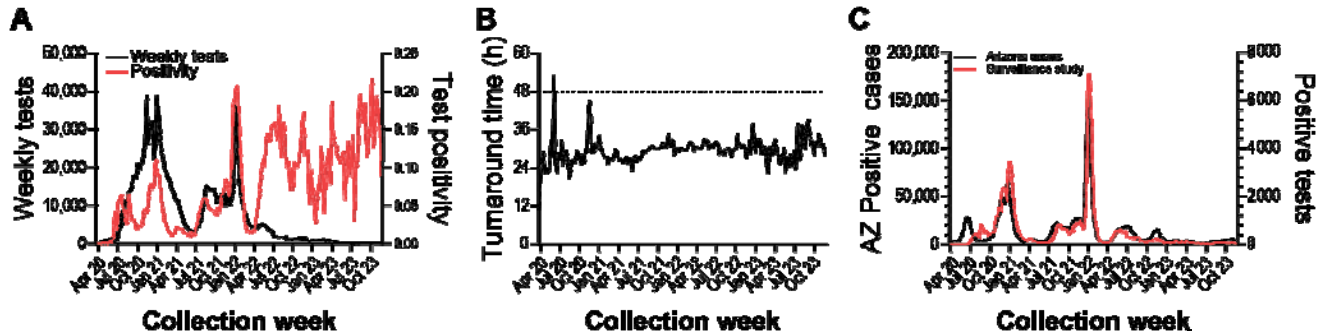
Characteristics	No.	(%)
<u>Total unique participants</u>	366681	
<u>Sex</u>		
Male	186090	(50.7)
Female	176649	(48.2)
Unknown	1457	(0.4)
Invalid, or no answer	2485	(0.7)
<u>Race</u>		
White	202398	(55.2)
Black or African American	20742	(5.7)
Asian	16355	(4.5)
American Indian or Alaska Native	13428	(3.7)
Native Hawaiian or other Pacific Islander	1435	(0.9)
Other	34149	(9.3)
Unknown	3455	(5.7)
Declined	15017	(4.1)
Invalid or no answer	59485	(16.2)
<u>Ethnicity</u>		
Not Hispanic or Latino	225704	(61.6)
Hispanic or Latino	80244	(21.9)
Unknown	7860	(2.1)
Declined	5960	(1.6)
Invalid or no answer	46913	(12.8)
<u>Age at first test</u>		
0-17	33346	(9.1)
18-21	77053	(21)
22-29	74638	(20.4)
30-39	64335	(17.5)
40-49	45621	(12.4)
50-59	36209	(9.9)
60+	34486	(9.4)
Invalid or no answer	993	(0.3)

286

287

288
289
290
291
292
293
294

Testing frequency was high during the initial surveillance period through 2022 but was greatly diminished throughout 2023 (Figure 2A). Generally, total testing was low in the summer months and higher during the academic school year. Test administration peaked in December 2020 and experienced another large rise in December 2021. Positivity rate fluctuated over the surveillance period, with peak positivity during January 2022. Interestingly, we observed that after July 2022, the positivity rate remained elevated compared to previous rates.



295
296
297
298
299

Figure 2. SARS-CoV-2 RT-PCR testing surveillance from April 2020 to November 2023. (a) Left axis: Weekly tests performed. Right axis: Weekly test positivity. (b) Average weekly test result turnaround time. (c) Left axis: Weekly Arizona SARS-CoV-2 case count. Right axis: Surveillance weekly positive samples.

300
301
302
303
304
305
306
307
308
309
310

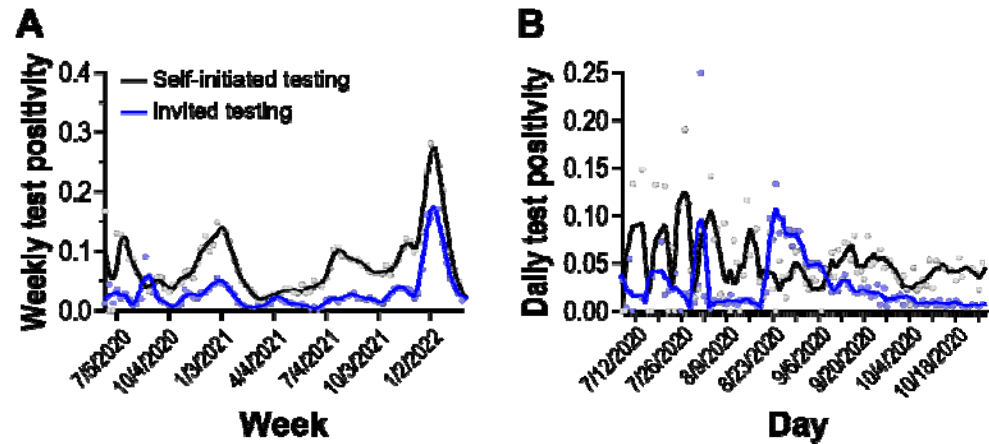
The median turnaround time from participant sample registration to electronic delivery of RT-PCR results was 29.2 hours, and weekly average turnaround times rarely exceeded 48 hours (Figure 2B). We wanted to determine if our surveillance strategy and response time was indicative of SARS-CoV-2 infection in the broader community, so we compared our weekly positive test counts to Arizona COVID19 case counts (Figure 2C). We found that trends between the two metrics were highly correlated (Pearson $r = 0.9073$, 95% CI: 0.88-0.93, $p < 0.0001$). Taken together, we observed that the diversity and responsiveness of our surveillance testing strategy sufficiently captured the local region's epidemiological status.

311

3.4. Randomly selected test participation detected infection outbreaks

312
313
314
315
316
317
318
319

Our surveillance program was comprised of community participants self-initiating testing as well as participants invited to test by an affiliate organization (e.g. school, employer), so we wanted to compare how positivity between self-initiated testing compared to a population randomly selected and invited to test. Through May 2020 and February 2022, we compared test positivity for an organization implementing randomized, invited testing to individuals self-initiating testing from the same geographic area. We observed that test positivity for self-initiated testing was generally higher than invited testing, but followed similar upward and downward trends (Figure 3A).



320
321 **Figure 3.** Test positivity rate of self-initiated and invited testing cohorts. Solid lines are 2nd order
322 smoothing functions across 3 neighbor data points. (a) Weekly test positivity during the surveil-
323 lance period. (b) Daily test positivity around outbreak period (see text).

324
325 Starting on August 22, 2020, we observed a period of 17 days where the invited
326 testing cohort displayed test positivity higher than the self-initiated testing cohort (**Fig-**
327 **ure 3B**). It took approximately 40 days for test positivity in the randomly selected invited
328 cohort to return to pre-elevated levels. Overall, we observed that randomly selected in-
329 vited testing can detect outbreaks not captured in self-initiated sampling strategies.

330
331 *3.5. Saliva sample collection enabled whole viral genome sequencing of clinical positives for ge-*
nomics epidemiology investigations

332 In order to monitor for the introduction of VOCs and the emergence of novel muta-
333 tions within circulating variants, whole viral genome sequencing of RT-PCR positive
334 participant samples was performed. Over the surveillance period, sequencing of 69,595
335 saliva samples was attempted and 54,040 consensus genome sequences received suffi-
336 cient coverage for PANGO designation and were submitted to the GISAID database
337 (**Table 3**).

338 From September 2020 through February 2021, saliva and nucleic acid extracts from
339 SARS-CoV-2 positive samples were stored at -80°C until sequencing infrastructure was
340 finalized. When NGS started in February 2021 through December 2021, weekly GISAID
341 submissions generally matched RT-PCR positive sample collections (**Figure 4A**). In late
342 December 2021 to February 2022, a surge of positive RT-PCR samples caused sample in-
343 flux to exceed sequencing capacity. Over this period, samples collected on the most re-
344 cent day were prioritized for WGS and others were banked for later sequencing. From
345 February 2022 to May 2022, GISAID submissions greatly surpassed sample collections.
346 During this period, banked samples were supplemented into NGS runs to meet se-
347 quencing capacity. After May 2022, GISAID submissions tracked sample collections and
348 overall sample collections decreased compared to earlier dates.

349 Sample sequencing turnaround time, the time between participant sample registra-
350 tion and GISAID submission, is important to maintaining a 'real-time' analysis of circu-
351 lating variants, therefore we analyzed the sample turnaround for our sequencing sam-
352 ples [28]. Turnaround time fluctuated over the surveillance period (**Figure 4B**). Samples
353 collected and banked before sequencing infrastructure was established in February 2021,
354 had the longest turnaround times. In May 2021, median turnaround times shortened to a
355 desired 7-14 day turnaround time. Median turnaround times increased during December

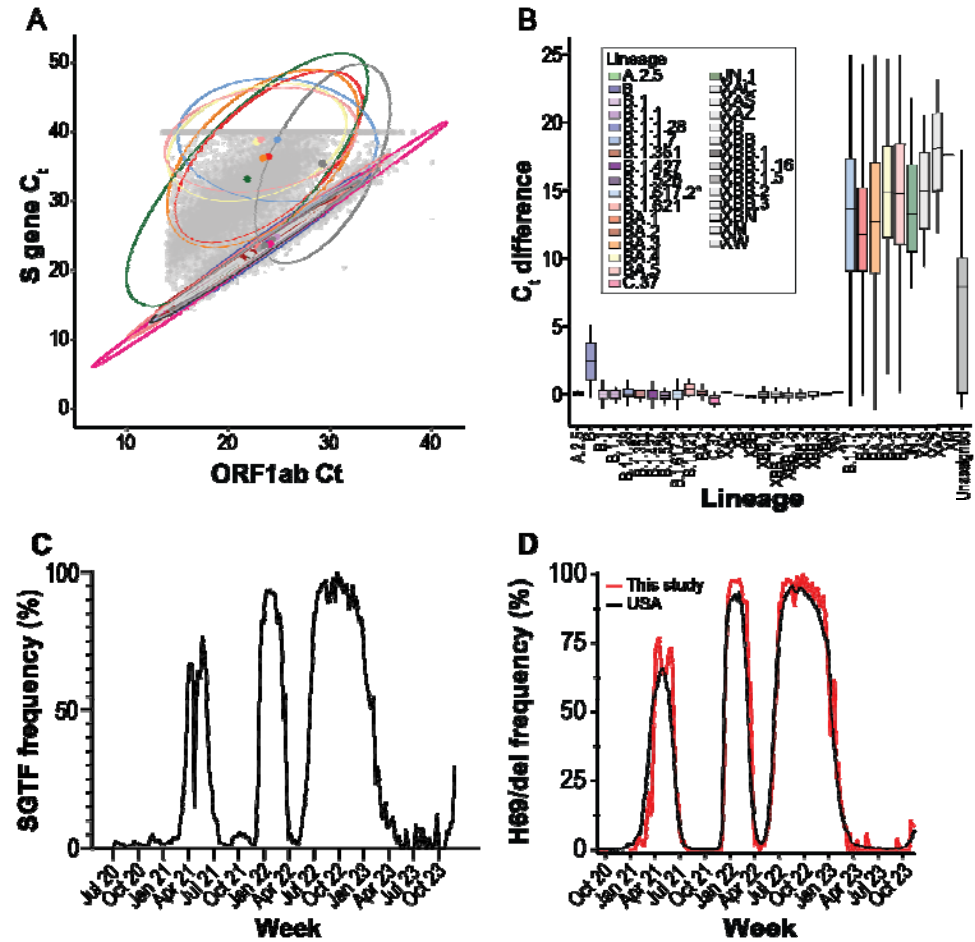
363 **Figure 4.** Whole viral genome sequencing of SARS-CoV-2 positive saliva samples. (a) Weekly
364 RT-PCR positive samples (line) and weekly GISAID submissions (bars). (b) GISAID collection to
365 submission turnaround time for surveillance program and other USA samples. Solid line corre-
366 sponds to median turnaround time. Bottom and top of boxes correspond to Q1 and Q3 values, re-
367 spectively. (c) Relative weekly abundance of SARS-CoV-2 PANGO lineages. (d) TaqPath Ct values
368 and consensus genome ambiguity of saliva samples. Blue line shows LOWESS smoothing of all
369 samples. (b)

370
371 In order to observe trends in SARS-CoV-2 virus evolution, we looked at the relative
372 abundances of each lineage using the GISAID lineage calls from our submitted samples
373 over the surveillance period (**Figure 4C**). Major lineages reaching a majority relative
374 abundance ($\geq 50\%$ of samples) in any week over the surveillance period were: B.1, B.1.1.7
375 (Alpha), B.1.617.2 (Delta, with AY sublineages), BA.1 (Omicron), BA.2 (Omicron), BA.3
376 (Omicron), BA.5 (Omicron), XBB.1 (Omicron-recombinant), XBB.1.5 (Omi-
377 cron-recombinant), XBB.1.16 (Omicron-recombinant). Notable lineages that were de-
378 tected but did not meet majority abundance were: A.2.5, B.1.1.28/P.1 (Gamma), B.1.351
379 (Beta), B.1.526 (Iota), B.1.621 (Mu), BA.4 (Omicron), C.37 (Lambda), and JN.1 (Omicron).
380 The following non-XBB.1 recombinant lineages were detected during the surveillance
381 period: XAC, XAS, XAZ, XB, XBB.2, XBB.3, XBN, XCM, XM, XW.

382 Finally, to assess the effect of viral load on sequencing performance, we compared
383 TaqPath C_t values to consensus genome ambiguity (**Figure 4D**). We observed that fewer
384 ambiguities were obtained at higher viral loads and ambiguity frequency rose as viral
385 load decreased. Performing a LOWESS regression of all samples found that C_t values
386 below 32.0 and 26.0 were associated with fewer than 30% and 5% ambiguities, respec-
387 tively. We observed a low frequency ($n = 998$, 1.7%) of genomes with less than 30% am-
388 biguity that failed pangolin lineage designation or GISAID acceptance. We also observed
389 that a low proportion ($n = 342$, 0.6%) of consensus genomes with over 30% ambiguities
390 were able to receive pangolin lineage designations and GISAID acceptance.

391 3.6. Diagnostic test failure allowed rapid genotyping of saliva samples

392 The TaqPath Combo Kit detects the presence of SARS-CoV-2 genomes using primers
393 and probes with homology to the ORF1ab, N, and S genes. When we compared Orf1ab
394 gene or N gene C_t values to S gene C_t values, we observed populations of genomes with
395 discordant S gene C_t values (**Figure 5A**). Genome sequencing revealed that this popula-
396 tion was primarily composed of specific lineages. Of the major, notable, and recombinant
397 lineages observed over the surveillance period (**Figure 4C**), we observed significantly
398 large differences in median TaqPath C_t values for B.1.1.7 (Alpha), BA.1 (Omicron), BA.3
399 (Omicron), BA.4 (Omicron), BA.5 (Omicron), JN.1 (Omicron), XAS, XAZ, and XM line-
400 ages compared to the B.1.1 lineage (**Figure 5B**; Tukey HSD, $p < 0.005$). Median Orf1ab C_t
401 values differed between lineages but were not large enough to account for the observed
402 differences (**Supplementary Figure S1**). The lineages displaying S gene target failure
403 (SGTF) all contain the H69del/V70del mutations.



404
405 **Figure 5.** S gene target failure (SGTF) on TaqPath COVID19 Combo Kit RT-PCR assays. (a) Mean
406 ORF1ab/N gene Ct values and S gene Ct values of positive saliva samples. Ellipses capture 95% of
407 samples belonging to each PANGO variant. Colored points indicate ellipse centroid. Lineage col-
408 oration is shared between panels (a) and (b). (b) Difference between S gene and mean ORF1ab/N
409 gene Ct values for PANGO variants displaying SGTF. The bottom, middle, and top of boxes cor-
410 respond to Q1, Q2, and Q3, respectively. Box whiskers correspond to the largest value no further
411 than 1.5*IQR. (c) Weekly SGTF prevalence in local samples. (d) Weekly abundance of samples
412 containing S:H69del mutation in USA and local samples.

413 We detected three periods of high SGTF frequency over the surveillance period, as
414 well as growing frequency at the end of the survey period (Figure 5C). We compared the
415 frequency of our sequenced genomes containing H69/V70 deletion to the frequency of
416 other USA genomes and observed that the mutation frequency patterns were identical to
417 SGTF frequency (Figure 5D). In summary, multiple times during the surveillance period,
418 RT-PCR diagnostic test failure enabled rapid H69/V70 deletion genotyping and facili-
419 tated a fast way to monitor changing lineage abundance.

421 4. Discussion

422 In this study we report the multi-year effort of monitoring the introduction and
423 evolution of SARS-CoV-2 in Tempe, Arizona. Self-collected saliva samples were an ad-
424 equate matrix for qualitative diagnosis of SARS-CoV-2 infection, and we obtained robust
425 genome sequencing from most positive samples. Using our surveillance system, we as-

426
427
428
429
430
431
432
433
434
435
436
437
438
439
440
441
442
443
444
445
446
447
448
449
450
451
452
453
454
455
456
457
458
459
460
461
462
463
464
465
466
467
468
469
470
471
472
473
474
475
476

sessed the epidemiological health of the community and monitored evolution of the SARS-CoV-2 virus throughout the pandemic.

Our multi-year surveillance was primarily located in an urban metropolitan area of a major US city. Due to the high testing volume, high sequencing depth, and fast turnaround times, our surveillance program provided a robust representation of SARS-CoV-2 epidemiology [28]. Variant introduction and abundance patterns that we observed concur with patterns seen in other regional studies [29]. Upward and downward trends in testing frequency and positivity also appear consistent with regional (Figure 1C) and national [30] case counts and test positivity. However, in this study, we observe an overall increase in test positivity dynamics before and after infections peaked during the Omicron BA.1 variant introduction in January 2022 (Figure 2A).

We also observed periods where self-initiated testing was higher than invited testing (Figure 3). Patterns of test positivity might be attributed to the motivations behind SARS-CoV-2 self-initiated testing. Testing motivations are multifaceted, involving personality, behavioral, clinical, and economic factors [31,32]. The availability of SARS-CoV-2 vaccines after December 2020 [33] may be also have contributed to altered testing motivations. Seroprevalence surveillance during this time period, showed a large number of adults had antibodies to SARS-CoV-2 through vaccination, infection, or both [34]. Attitudes to testing may have been altered due to perceived protection status from vaccination or naturally acquired immunity (i.e., recent infection). Finally, the increased availability of commercial, at-home, SARS-CoV-2 tests may have altered the surveillance population and their motivations. Our study shows that while self-initiated and invited testing are generally in concordance, further understanding of testing motivations and how to promote self-initiated testing may improve the representativeness of self-initiated testing.

Co-localizing RT-PCR and WGS operations resulted in valuable benefits. Close physical proximity reduced sample transit and storage time, minimized the number of freeze-thaw cycles a sample was exposed to, and facilitated communication between teams. Shipping time, storage time, and freeze-thaw cycles are all factors that negatively affect RNA stability [35]. Enhanced communication and coordination abilities allowed catching and correcting errors, as well as assisted in coordinating sequencing priority based on SGTF results.

In addition to internal communication, external guidance by state and federal agencies provided valuable information. The US Food & Drug Administration guidance documents assisted in the development of the Arizona Biodesign Clinical Testing Lab and establishing our surveillance program [36]. Federal agencies also organized regular status and discussion panels, such as the CDC's Sequencing for Public Health Emergency Response, Epidemiology, and Surveillance (SPHERES) consortium [37]. These supplementary communication networks facilitated prompt dispersal of information between testing sites, such as when novel variants displayed reduced sensitivity to diagnostic assays.

The genetic determinants of SGTF were known soon after introduction of the Alpha variant [12]. The H69del/V70del mutation in the Spike protein provides no immune escape properties itself but rescues other Spike protein mutations with increased antibody evasion but impaired infectivity [38]. The increased prevalence of SGTF on SARS-CoV-2 specimens led to the design and adoption of TaqPath 2.0 for primary diagnostic use. However, the continued use of the TaqPath Combo Kit Assay continued to provide important public health data. Broadly, it allowed facilities without sequencing capabilities to monitor variant introduction [39]. SGTF provided fast variant typing during the Alpha-Delta, Delta-Omicron BA.1, Omicron BA.1-Omicron BA.2, Omicron BA.2-Omicron BA.3/4/5, and Omicron BA.3/4/5-XBB transitions (Figures 4C and 5A). For sequencing

477 laboratories, SGTf was useful when sample positivity exceeded sequencing capacity, as
478 it allowed researchers to direct sequencing efforts towards samples suspected of being
479 newly introduced variants. Subsequent WGS allowed confirmation of those variants and
480 allowed surveillance for novel mutations within introduced lineages.

481 Although most samples with low genome ambiguity were accepted for database
482 submission, we observed a small number ($n = 979$, 1.4%) of samples that had high ge-
483 nome coverage ($>30\%$) but failed lineage designation or GISAID submission (Figure 4D).
484 Within our workflow, submission of consensus genomes to the GISAID database was
485 conditional upon assignment of a PANGO lineage by pangolin software at the time of
486 sequencing analysis. Further, samples with contamination or true co-infection may have
487 received mixed-lineage designations and been excluded from database submission.
488 There may also be some cases where a sample contained ambiguities at nucleotides crit-
489 ical in lineage designation or samples belonged to undesignated lineages at the time of
490 analysis. Amplicon-based sequencing was the primary sequencing method, therefore
491 mutations in viral genomes located within primer binding regions would cause reduced
492 sequencing coverage of that amplicon. This phenomenon, termed amplicon drop-out, has
493 occurred multiple times over the course of SARS-CoV-2 evolution [40,41]. Samples with
494 ambiguities in positions critical to lineage defining specificity may have been incorrectly
495 assigned a lineage or left unassigned, causing them to fail submission. During our study,
496 we obtained genome completeness scores, with respect to RT-PCR Ct values, comparable
497 to those observed in another study [42], illustrating that saliva is a viable medium for
498 robust, large scale genomic surveillance.

499 Ultimately, in this study we determined that self-collected saliva-based surveillance
500 assays can provide important epidemiological information during a public health crisis.
501 We observed that our surveillance system (i) provided an effective means to broadly as-
502 sess community health and epidemic status, (ii) provided a means to effectively detect
503 outbreaks within the population to target remediation strategies, and (iii) quickly pro-
504 vided high-quality material to enable the monitoring of pathogen evolution by WGS
505 during an epidemic crisis. Due to its simple collection and low invasiveness, continued
506 examination of saliva as a testing matrix for routine and pandemic pathogen surveillance
507 is important.
508

509 **Supplementary Materials:** The following supporting information can be downloaded at:
510 <https://www.mdpi.com/article/doi/s1>, Figure S1: TaqPath COVID-19 Combo Kit Orflab Ct values
511 of saliva samples by SARS-CoV-2 lineages; Table S1: Limit of detection analysis of SARS-CoV-2
512 detection in nasopharyngeal swabs using the TaqPath COVID-19 Combo Kit qPCR assay.

513 **Author Contributions:** Conceptualization, V.M., J.L., and E.S.L.; methodology, T.R., V.M., I.S and
514 E.S.L.; software, I.S., and S.H.; formal analysis, S.H and V.M.; data curation, S.H.; writing—original
515 draft preparation, S.H.; writing—review and editing, S.H., V.M., and J.L.; visualization, S.H.; su-
516 pervision, C.C. and V.M.; project administration, V.M.; funding acquisition, V.M., E.S.L., and J.L.
517 All authors have read and agreed to the published version of the manuscript." Please turn to the
518 CRediT taxonomy for the term explanation. Authorship must be limited to those who have con-
519 tributed substantially to the work reported.

520 **Funding:** This research was funded by the Virginia G. Piper foundation, Arizona State University
521 Knowledge Enterprise, Arizona State Department of Health Services (CTR053916), U.S. Centers for
522 Disease Control and Prevention (CDC BAA 75D30121C11084), and Tohono O'odham Nation
523 (2020-01 ASU).

524 **Institutional Review Board Statement:** Ethical review and approval were waived for this study
525 due to the use of deidentified samples; metadata did not include any participant-identifiable in-
526 formation.

527 **Informed Consent Statement:** Not applicable.

528 **Data Availability Statement:** Viral genome sequences generated in this surveillance program were
529 submitted to the GISAID nCov database and can be obtained using the EPI_SET ID:
530 EPI_SET_250224ka. RT-PCR results, sequencing results, and patient metadata is available at
531 DataDryad: <https://doi.org/10.5061/dryad.z08kprsh>

532 **ASU Biodesign Clinical Testing Lab (ABCTL) Diagnostic and Sequencing Teams** (alphabetical
533 listing): Ajeet Bains, Bradley Bobbett, Veronica Boyle, Sean Dudley, Alexis Emerson, Michael
534 Fiacco, Izamer Garcia, Kristina Gonzalez-Wartz, Akshaya Gunasekaran, Valerie Harris, LaRinda A.
535 Holland, Ching-Wen Hou, James C. Hu, Preston Hunter, Nathaniel Johnson, Emily A. Kaelin, Mark
536 Knappenberger, Victoria R. Leonard, Kyle Lewis, Jessica Lukosus, Madhuranga Thilakasiri
537 Madugoda Ralalage Don, Mitch Magee, Shodhan Manda, Rabia Maqsood, Winston Matthews,
538 Aaron McDonald, Tianchen Mu, Advait Murugan, Nicholas Nabours, Benjamin Nussel, Yasmine
539 Parra, Peter Patterson, Nghia C. Pham, Eric Reamer, Michael Ritchie, Tyler Schroeder, Amit
540 Arunkumar Sharma, Peter T. Skidmore, Matthew F. Smith, Regan A. Sullins, Alexis Thomas, An
541 Tieu, Kevin Tinnin, and Chau Tran, Lily I. Wu.

542 **Conflicts of Interest:** The authors declare no conflicts of interest. The funders had no role in the
543 design of the study; in the collection, analyses, or interpretation of data; in the writing of the man-
544 uscript; or in the decision to publish the results.

545 **Abbreviations**

546 The following abbreviations are used in this manuscript:

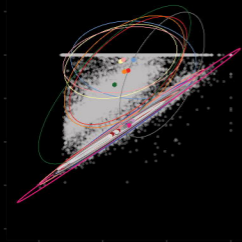
(S)GTF	(S) Gene Target Failure
CDC	Centers for Disease Control and Prevention
COVID-19	Coronavirus disease 2019
EUA	Emergency Use Authorization
GISAID	Global Initiative on Sharing All Influenza Data
HIPAA	Health Insurance Portability and Accountability Act
LOWESS/LOESS	Locally Weighted/Estimated Scatterplot Smoothing
NGS	Next-generation sequencing
NPA	nasopharyngeal aspirate
NPS	nasopharyngeal swab
PANGO(LIN)	Phylogenetic Assignment of Named Global Outbreak (Lineages)
RT-PCR	reverse transcriptase polymerase chain reaction
SARS-CoV-2	Severe acute respiratory syndrome coronavirus 2
VOC	Variant of Concern
VOI	Variant of Interest
VUM	Variant Under Monitoring
WGS	Whole Genomes Sequencing
WHO	World Health Organization

547 **References**

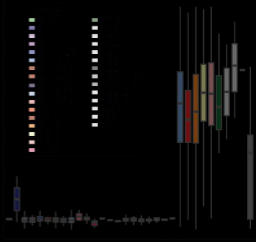
- 548 1. Wu, F.; Zhao, S.; Yu, B.; Chen, Y.M.; Wang, W.; Song, Z.G.; Hu, Y.; Tao, Z.W.; Tian, J.H.; Pei, Y.Y.; et al. A new coronavirus
549 associated with human respiratory disease in China. *Nature* **2020**, 579, 265-269, doi:10.1038/s41586-020-2008-3.
- 550 2. World Health Organization. WHO Director-General's statement on IHR Emergency Committee on Novel Coronavirus
551 (2019-nCoV). Available online:
552 [https://www.who.int/director-general/speeches/detail/who-director-general-s-statement-on-ihr-emergency-committee-on-](https://www.who.int/director-general/speeches/detail/who-director-general-s-statement-on-ihr-emergency-committee-on-novel-coronavirus-(2019-ncov))
553 [novel-coronavirus-\(2019-ncov\)](https://www.who.int/director-general/speeches/detail/who-director-general-s-statement-on-ihr-emergency-committee-on-novel-coronavirus-(2019-ncov)) (accessed on 2 February).
- 554 3. World Health Organization. Statement on the fifteenth meeting of the IHR (2005) Emergency Committee on the COVID-19
555 pandemic. Available online:
556 [https://www.who.int/news/item/05-05-2023-statement-on-the-fifteenth-meeting-of-the-international-health-regulations-\(20](https://www.who.int/news/item/05-05-2023-statement-on-the-fifteenth-meeting-of-the-international-health-regulations-(2005)-emergency-committee-regarding-the-coronavirus-disease-(covid-19)-pandemic)
557 [05\)-emergency-committee-regarding-the-coronavirus-disease-\(covid-19\)-pandemic](https://www.who.int/news/item/05-05-2023-statement-on-the-fifteenth-meeting-of-the-international-health-regulations-(2005)-emergency-committee-regarding-the-coronavirus-disease-(covid-19)-pandemic) (accessed on 2 February).
- 558 4. Johns Hopkins University & Medicine. COVID-19 Dashboard. Available online: <https://coronavirus.jhu.edu/map.html>
559 (accessed on 2 February).
- 560 5. Frazee, B.W.; Rodriguez-Hoces de la Guardia, A.; Alter, H.; Chen, C.G.; Fuentes, E.L.; Holzer, A.K.; Lolas, M.; Mitra, D.;
561 Vohra, J.; Dekker, C.L. Accuracy and Discomfort of Different Types of Intranasal Specimen Collection Methods for
562 Molecular Influenza Testing in Emergency Department Patients. *Ann Emerg Med* **2018**, 71, 509-517 e501,
563 doi:10.1016/j.annemergmed.2017.09.010.
- 564 6. To, K.K.W.; Yip, C.C.Y.; Lai, C.Y.W.; Wong, C.K.H.; Ho, D.T.Y.; Pang, P.K.P.; Ng, A.C.K.; Leung, K.H.; Poon, R.W.S.; Chan,
565 K.H.; et al. Saliva as a diagnostic specimen for testing respiratory virus by a point-of-care molecular assay: a diagnostic
566 validity study. *Clin Microbiol Infect* **2019**, 25, 372-378, doi:10.1016/j.cmi.2018.06.009.
- 567 7. Azzi, L.; Carcano, G.; Gianfagna, F.; Grossi, P.; Gasperina, D.D.; Genoni, A.; Fasano, M.; Sessa, F.; Tettamanti, L.; Carinci,
568 F.; et al. Saliva is a reliable tool to detect SARS-CoV-2. *J Infect* **2020**, 81, e45-e50, doi:10.1016/j.jinf.2020.04.005.
- 569 8. Uddin, M.K.M.; Shirin, T.; Hossain, M.E.; Alam, A.N.; Ami, J.Q.; Hasan, R.; Miah, M.; Shaly, N.J.; Ahmed, S.; Rahman,
570 S.M.M.; et al. Diagnostic Performance of Self-Collected Saliva Versus Nasopharyngeal Swab for the Molecular Detection
571 of SARS-CoV-2 in the Clinical Setting. *Microbiol Spectr* **2021**, 9, e0046821, doi:10.1128/Spectrum.00468-21.
- 572 9. Lu, X.; Wang, L.; Sakthivel, S.K.; Whitaker, B.; Murray, J.; Kamili, S.; Lynch, B.; Malapati, L.; Burke, S.A.; Harcourt, J.; et al.
573 US CDC Real-Time Reverse Transcription PCR Panel for Detection of Severe Acute Respiratory Syndrome Coronavirus 2.
574 *Emerg Infect Dis* **2020**, 26, 1654-1665, doi:10.3201/eid2608.201246.
- 575 10. U.S. Food & Drug Administration. EUA200010. **2021**.
- 576 11. Holland, S.C.; Bains, A.; Holland, L.A.; Smith, M.F.; Sullins, R.A.; Mellor, N.J.; Thomas, A.W.; Johnson, N.; Murugan, V.;
577 Lim, E.S. SARS-CoV-2 Delta Variant N Gene Mutations Reduce Sensitivity to the TaqPath COVID-19 Multiplex Molecular
578 Diagnostic Assay. *Viruses* **2022**, 14, doi:10.3390/v14061316.
- 579 12. Public Health England. *Investigation of novel SARS-COV-2 variant: Variant of Concern 202012/01*; 21 December 2020 2020.
- 580 13. U.S. Food & Drug Administration. EUA210384. **2021**.
- 581 14. ThermoFisher Scientific. The Next Generation of COVID-19 Testing. Available online:
582 <https://www.thermofisher.com/blog/clinical-conversations/the-next-generation-of-covid-19-testing/> (accessed on 2
583 February).
- 584 15. Quick, J.; Grubaugh, N.D.; Pullan, S.T.; Claro, I.M.; Smith, A.D.; Gangavarapu, K.; Oliveira, G.; Robles-Sikisaka, R.; Rogers,
585 T.F.; Beutler, N.A.; et al. Multiplex PCR method for MinION and Illumina sequencing of Zika and other virus genomes
586 directly from clinical samples. *Nat Protoc* **2017**, 12, 1261-1276, doi:10.1038/nprot.2017.066.
- 587 16. ARTICnetwork. artic-nCoV-2019. Available online: <https://github.com/artic-network/artic-ncov2019> (accessed on 1
588 February 2025).
- 589 17. Rambaut, A.; Holmes, E.C.; O'Toole, A.; Hill, V.; McCrone, J.T.; Ruis, C.; du Plessis, L.; Pybus, O.G. A dynamic
590 nomenclature proposal for SARS-CoV-2 lineages to assist genomic epidemiology. *Nat Microbiol* **2020**, 5, 1403-1407,
591 doi:10.1038/s41564-020-0770-5.

-
- 592 18. Konings, F.; Perkins, M.D.; Kuhn, J.H.; Pallen, M.J.; Alm, E.J.; Archer, B.N.; Barakat, A.; Bedford, T.; Bhiman, J.N.; Caly, L.;
593 et al. SARS-CoV-2 Variants of Interest and Concern naming scheme conducive for global discourse. *Nat Microbiol* **2021**, *6*,
594 821-823, doi:10.1038/s41564-021-00932-w.
- 595 19. World Health Organization. *Updated working definitions and primary actions for SARS-CoV-2 variants*; 4 October 2023.
- 596 20. Kruegar, F. Trim Galore. Available online: https://www.bioinformatics.babraham.ac.uk/projects/trim_galore/ (accessed on
597 2 February).
- 598 21. Martin, M. Cutadapt removes adapter sequences from high-throughput sequencing reads. *2011* **2011**, *17*, *3*,
599 doi:10.14806/ej.17.1.200.
- 600 22. Andrews, S. FastQC. Available online: <https://www.bioinformatics.babraham.ac.uk/projects/fastqc/> (accessed on 2
601 February).
- 602 23. Li, H.; Durbin, R. Fast and accurate short read alignment with Burrows-Wheeler transform. *Bioinformatics* **2009**, *25*,
603 1754-1760, doi:10.1093/bioinformatics/btp324.
- 604 24. Castellano, S.; Cestari, F.; Faglioni, G.; Tenedini, E.; Marino, M.; Artuso, L.; Manfredini, R.; Luppi, M.; Trenti, T.; Tagliafico,
605 E. iVar, an Interpretation-Oriented Tool to Manage the Update and Revision of Variant Annotation and Classification.
606 *Genes (Basel)* **2021**, *12*, doi:10.3390/genes12030384.
- 607 25. Li, H.; Handsaker, B.; Wysoker, A.; Fennell, T.; Ruan, J.; Homer, N.; Marth, G.; Abecasis, G.; Durbin, R.; Genome Project
608 Data Processing, S. The Sequence Alignment/Map format and SAMtools. *Bioinformatics* **2009**, *25*, 2078-2079,
609 doi:10.1093/bioinformatics/btp352.
- 610 26. O'Toole, A.; Scher, E.; Underwood, A.; Jackson, B.; Hill, V.; McCrone, J.T.; Colquhoun, R.; Ruis, C.; Abu-Dahab, K.; Taylor,
611 B.; et al. Assignment of epidemiological lineages in an emerging pandemic using the pangolin tool. *Virus Evol* **2021**, *7*,
612 veab064, doi:10.1093/ve/veab064.
- 613 27. Schaffer, A.A.; Hatcher, E.L.; Yankie, L.; Shonkwiler, L.; Brister, J.R.; Karsch-Mizrachi, I.; Nawrocki, E.P. VADR: validation
614 and annotation of virus sequence submissions to GenBank. *BMC Bioinformatics* **2020**, *21*, 211,
615 doi:10.1186/s12859-020-3537-3.
- 616 28. Brito, A.F.; Semenova, E.; Dudas, G.; Hassler, G.W.; Kalinich, C.C.; Kraemer, M.U.G.; Ho, J.; Tegally, H.; Githinji, G.; Agoti,
617 C.N.; et al. Global disparities in SARS-CoV-2 genomic surveillance. *Nat Commun* **2022**, *13*, 7003,
618 doi:10.1038/s41467-022-33713-y.
- 619 29. Jung, A.; Droit, L.; Febles, B.; Fronick, C.; Cook, L.; Handley, S.A.; Parikh, B.A.; Wang, D. Tracking the prevalence and
620 emergence of SARS-CoV-2 variants of concern using a regional genomic surveillance program. *Microbiol Spectr* **2024**, *12*,
621 e0422523, doi:10.1128/spectrum.04225-23.
- 622 30. Santos, S.; Humbard, M.; Lambrou, A.S.; Lin, G.; Padilla, Y.; Chaitram, J.; Natrajan, M.S.; Kirking, H.L.; Courtney, S.; Del
623 Guercio, K.; et al. The SARS-CoV-2 test scale-up in the USA: an analysis of the number of tests produced and used over
624 time and their modelled impact on the COVID-19 pandemic. *Lancet Public Health* **2025**, *10*, e47-e57,
625 doi:10.1016/S2468-2667(24)00279-2.
- 626 31. Perry, B.L.; Aronson, B.; Railey, A.F.; Ludema, C. If you build it, will they come? Social, economic, and psychological
627 determinants of COVID-19 testing decisions. *PLoS One* **2021**, *16*, e0252658, doi:10.1371/journal.pone.0252658.
- 628 32. Thunström, L.; Ashworth, M.; Shogren, J.F.; Newbold, S.; Finnoff, D. Testing for COVID-19: willful ignorance or selfless
629 behavior? *Behavioural Public Policy* **2020**, *5*, 135-152, doi:10.1017/bpp.2020.15.
- 630 33. U.S. Food & Drug Administration. Emergency Use Authorization (EUA) for emergency use of Pfizer-BioNTech COVID-19
631 Vaccine for the prevention of COVID-19. **2020**.
- 632 34. Hou, C.W.; Williams, S.; Trivino-Soto, G.; Boyle, V.; Rainford, D.; Vicino, S.; Magee, M.; Chung, Y.; LaBaer, J.; Murugan, V.
633 The omicron variant of SARS-CoV-2 drove broadly increased seroprevalence in a public university setting. *PLOS Glob*
634 *Public Health* **2025**, *5*, e0003893, doi:10.1371/journal.pgph.0003893.

-
- 635 35. Granados, A.; Petrich, A.; McGeer, A.; Gubbay, J.B. Measuring influenza RNA quantity after prolonged storage or
636 multiple freeze/thaw cycles. *J Virol Methods* **2017**, *247*, 45-50, doi:10.1016/j.jviromet.2017.05.018.
- 637 36. U.S. Food & Drug Administration. FDA Guidance Documents. Available online:
638 <https://www.fda.gov/regulatory-information/search-fda-guidance-documents> (accessed on January 1, 2025).
- 639 37. Prevention, U.S.C.f.D.C.a. SPHERES. Available online:
640 <https://www.cdc.gov/advanced-molecular-detection/php/spheres/index.html> (accessed on January 1, 2025).
- 641 38. Meng, B.; Kemp, S.A.; Papa, G.; Datir, R.; Ferreira, I.; Marelli, S.; Harvey, W.T.; Lytras, S.; Mohamed, A.; Gallo, G.; et al.
642 Recurrent emergence of SARS-CoV-2 spike deletion H69/V70 and its role in the Alpha variant B.1.1.7. *Cell Rep* **2021**, *35*,
643 109292, doi:10.1016/j.celrep.2021.109292.
- 644 39. Clark, C.; Schrecker, J.; Hardison, M.; Taitel, M.S. Validation of reduced S-gene target performance and failure for rapid
645 surveillance of SARS-CoV-2 variants. *PLoS One* **2022**, *17*, e0275150, doi:10.1371/journal.pone.0275150.
- 646 40. Itokawa, K.; Sekizuka, T.; Hashino, M.; Tanaka, R.; Kuroda, M. Disentangling primer interactions improves SARS-CoV-2
647 genome sequencing by multiplex tiling PCR. *PLoS One* **2020**, *15*, e0239403, doi:10.1371/journal.pone.0239403.
- 648 41. Ulhuq, F.R.; Barge, M.; Falconer, K.; Wild, J.; Fernandes, G.; Gallagher, A.; McGinley, S.; Sugadol, A.; Tariq, M.; Maloney,
649 D.; et al. Analysis of the ARTIC V4 and V4.1 SARS-CoV-2 primers and their impact on the detection of Omicron BA.1 and
650 BA.2 lineage-defining mutations. *Microb Genom* **2023**, *9*, doi:10.1099/mgen.0.000991.
- 651 42. Schnaubelt, A.T.; Brett-Major, D.M.; Williamson, J.; Barcal, B.; Carstens, J.; Peer, A.; Wiley, M.; Broadhurst, M.J.
652 SARS-CoV-2 genomic surveillance using self-collected saliva specimens during occupational testing programs. *Front*
653 *Public Health* **2025**, *13*, 1360862, doi:10.3389/fpubh.2025.1360862.

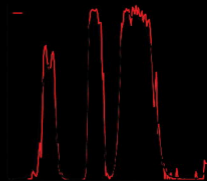


ORF1501



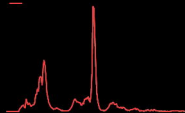
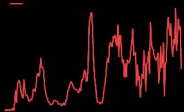
Language

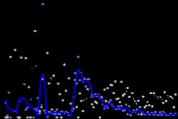
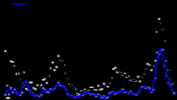
Normalized frequency



Week







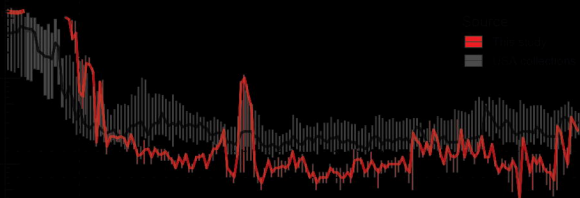
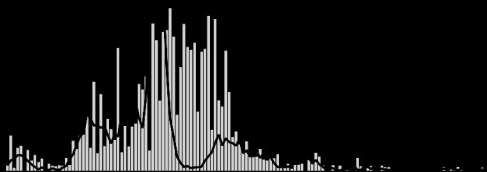


Figure 10.10.10

